# Dual-aperture fiber nulling for high spatial and spectral resolution studies of exoplanets

Anusha Pai Asnodkar<sup>a</sup>, Ji Wang<sup>a</sup>, Colby Jurgenson<sup>b</sup>, and Jonathan Crass<sup>a</sup>

<sup>a</sup>Department of Astronomy, The Ohio State University, 140 W. 18th Avenue, Columbus, OH 43210, USA;

<sup>b</sup>Harvard-Smithsonian Center for Astrophysics, 60 Garden St, Cambridge, MA, 02138, USA

## ABSTRACT

We are developing a "dual-aperture fiber nuller" (DAFN) as a technology to bridge the gap in observation of exoplanets with orbital separations between 1-10s of AU. Such an instrument interferometrically achieves an on-axis (starlight) null while off-axis light (planet light) is transmitted to a high-resolution spectrograph. The performance of the DAFN is competitive among only a few existing technologies such as the vortex fiber nuller. Furthermore, it has the cost-effective advantage of improving angular resolution by expanding the interferometric baseline rather than increasing aperture size. We present a monochromatic demonstration of this technology's angular resolution ( $< 1 \lambda/D$ ) and sensitivity to starlight suppression in the lab. The DAFN technology can potentially be deployed to preexisting interferometric frameworks such as the Large Binocular Telescope Interferometer or the Very Large Telescope Interferometer. It can also benefit prospective space-based exoplanet direct imaging missions, e.g. LIFE, as well as ground-based ELT searches for terrestrial planets in the habitable zone.

Keywords: Exoplanets, Interferometry, High Dispersion Coronagraphy, Fiber Nulling

#### 1. INTRODUCTION

Spectroscopic characterization of exoplanet atmospheres reveals key insights into their weather, compositional tracers of planet formation and evolution, and potential biosignatures. At present, exoplanet spectroscopy is limited to: 1) transiting planets and 2) directly imaged planets. Both populations of planets are shown in Figure 1. Notably there is a gap in parameter space between these two observation techniques, and even within the two populations, not all planets have properties amenable to spectroscopic detection of their atmospheres. For example, transiting planets with observed spectral features predominantly range from highly-irradiated sub-Neptunes to hot/warm Jupiters with current capabilities, even though we can observe the transits of super-Earths. Spectroscopy of directly imaged planets is largely performed on young super-Jupiters emitting significant residual thermal radiation from initial formation. Moreover, analogs to planets in our solar system currently are not accessible spectroscopically. They are too far from their hosts to be statistically likely to transit and furthermore are too cold to have large enough scale heights for their atmospheres to be detected via transmission/emission spectroscopy. They are also too faint and within the inner working angle of many coronagraphic technologies to be directly imaged.

To bridge the gap in parameter space and bring solar system analogs within reach of spectroscopic characterization, nulling interferometry employs long-baseline beam combination to achieve starlight suppression at high spatial resolution. Originally proposed as a two-aperture rotating baseline configuration for exoplanet detection, this concept has grown as the modes of interferometry have expanded with new optical technologies like the vortex phase mask and the phase knife. At its core, nulling interferometry requires pupil-plane phase modulation (e.g. phase offset of  $\pi$  for the two-aperture configuration) and beam combination to impose destructive interference over a target star, suppressing its light while off-axis light from an orbiting planet constructively interferes to produce a detectable signal. This inspired mission concepts like ESA's Darwin<sup>2</sup> and NASA's Terrestrial Planet Finder Interferometer.<sup>3</sup> The Palomar Fiber Nuller<sup>4</sup> (PFN) successfully demonstrated this concept with

Send correspondence to paiasnodkar.1@osu.edu

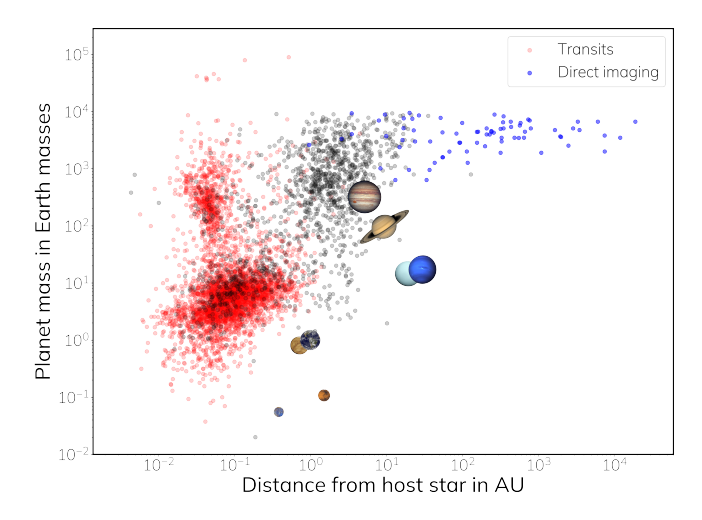


Figure 1. Population of all known exoplanets in mass vs. orbital separation space, with transiting and directly imaged planets highlighted. Note that this figure highlights *all* transiting and directly imaged planets, not just the ones which have been observed with spectroscopy.

sub-aperture pupil masking to achieve on-sky near-infrared (NIR) null depths down to  $1.6 \times 10^{-4}$  and detections of faint stellar companions within the diffraction limit.<sup>5</sup>

Fiber nulling focuses the interference pattern onto a single mode fiber (SMF), which performs additional suppression of stellar modal noise and simultaneously can serve as a spatial filter for spectroscopy. In addition to the PFN, the Keck Planet Imager and Characterizer (KPIC) instrument can perform fiber nulling with its vortex fiber nulling (VFN) mode, where phase modulation is performed by a vortex (continuous) phase ramp instead of two apertures with path lengths differing by a half-wave. This VFN mode of KPIC has achieved on-sky starlight rejection of  $\sim 10^{-2}$  in the K-band.<sup>6</sup>

We are developing a testbed for a dual-aperture fiber nuller (DAFN). The DAFN instrument concept is directly relevant to the Large Binocular Telescope (LBT) with its intrinsic interferometric capabilities combining two 8.4-m apertures on a common mount and edge-to-edge baseline of 22.8 m. This has a few advantages over VFN, such as higher throughput and an azimuthally asymmetric PSF for angular sensitivity to the position of a planet orbiting its host star. Furthermore, DAFN does not require throwing out light like PFN with its two subapertures, and, for a facility like the LBT, has a longer physical baseline than the cross-aperture interferometry employed by VFN and PFN. This testbed can be extended in the future to assess different multi-aperture fiber nulling paradigms, generalizing its applications to other facilities like the Very Large Telescope (VLT).

In this paper, we describe the DAFN concept and our testbed implementation in §2. §3 highlights the preliminary results from our fiber nulling experiment, and §4 outlines ongoing and future efforts to improve DAFN performance in our optical monochromatic demonstration as well as extend it to broadband and NIR wavelengths.

## 2. METHODS

The DAFN concept is explored in great detail in Ref. 7, in which Figure 1 provides a visual depiction of the design. A two-aperture telescope is pointed at a stellar source. The two beams are offset in phase by  $\pi$  at a pupil plane before they are focused onto a SMF. Due to the phase offset, the beams destructively interfere the light from the star to produce a dark fringe on-axis or a "null". Off-axis light (from a companion planet) will still constructively interfere and at the appropriate angular separations ( $\lesssim 1 \ \lambda/D$ ), these bright fringes can couple into the fiber. The fiber acts as the beam combining element for the interference of the two beams and directs the light to a high-resolution spectrograph for atmospheric characterization. In this manner, the DAFN performs high dispersion coronagraphy in three steps. First, nulling interferometry of the light from the two apertures executes the dominant mode of starlight suppression. Next, the SMF conducts spatial filtering and rejects modal

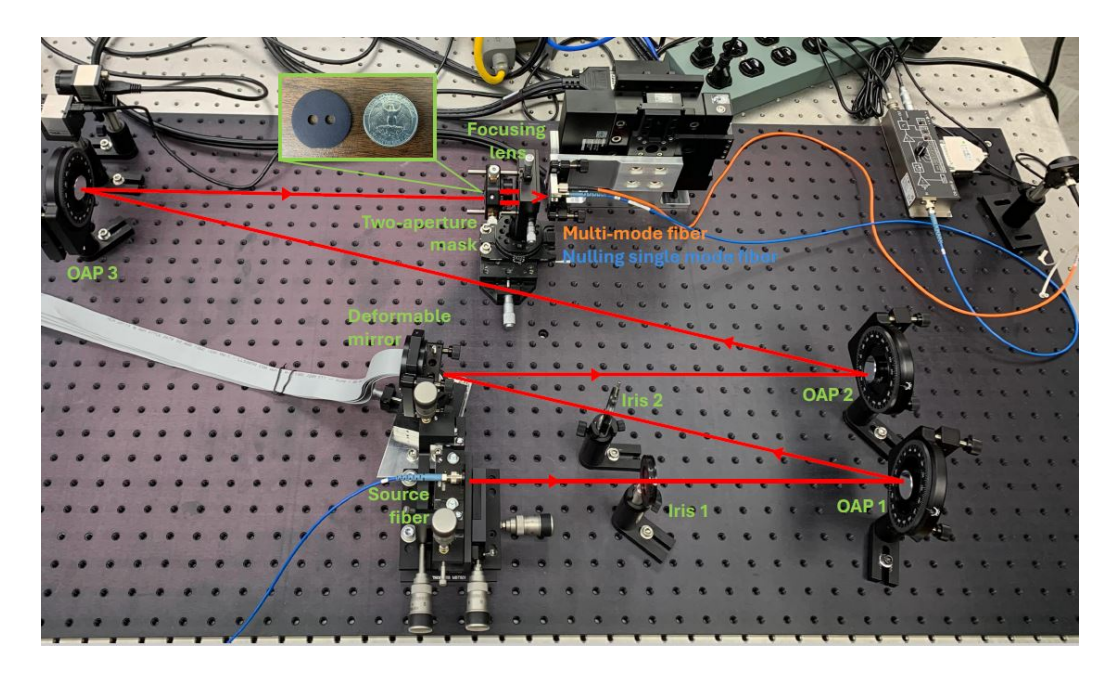


Figure 2. Testbed for monochromatic demonstration of DAFN.

noise (e.g. stellar speckles) that do not couple to the fundamental mode of the fiber. Finally, high-resolution spectroscopy further distinguishes planet light from starlight since the planet's spectral features shift in velocity space due to the planet's orbital motion while the stellar spectrum remains relatively stationary. The potential to attain sub- $\lambda/D$  coronagraphy makes the DAFN a suitable candidate for observing solar system analog giants within the inner working angles currently achieved by high contrast technologies.

Figure 2 displays our optical testbed. The optical path begins with a 635 nm laser source (Thorlabs S1FC635PM, not pictured) at the bottom left. The light is collimated by the first off-axis parabola mirror (OAP), OAP1 (all OAPs in our testbed are 1" diameter, 387.6 mm EFL Edmund Optics 35-538). There is a deformable mirror (DM; a Boston Micromachines Multi-DM purchased as Thorlabs DM140A-35-UP01) for wavefront control in collimated space. The pupil plane is reimaged with OAP2 and OAP3, where a custom two-aperture mask is placed; this mask was designed to emulate the aperture-to-baseline ratio of the LBT. A scalar phase-knife is applied to the DM such that half of the surface is offset with an optical path delay by  $\pi$  in phase relative to the other half, resulting in the two beam paths after the two-aperture mask to be out-of-phase and producing a central dark fringe when they are interfered. In our setup, the DM serves as a means of both phase modulation and wavefront correction. The two beams are focused with an aspheric lens (Edmund 85-301) onto the SMF (Thorlabs P1-630PM-FC-2), which is mounted on an automated 3-axis translation stage (Zaber LDA-AE XYZ) with manual tip-tilt adjustment (Thorlabs KM100S). The SMF is connected to an optical photodetector (FEMTO OE-200-SI-FC) with adjustable gain for measuring fiber throughput across a broad dynamic range. The photodetector's signal is read out with a PC USB oscilloscope (PicoScope 2204A) for analog to digital conversion. An optical multimode fiber (Thorlabs M43L01) is also placed on a common mount with the SMF and is read out with the photodetector at the position of maximum coupling for throughput normalization.

To minimize optical aberrations in the system, we scan the fiber along all 3 spatial dimensions to find where coupling into the SMF is maximized and incrementally perform mechanical alignment (without the two-aperture mask and phase knife implemented) to increase throughput. Additionally, we conduct Zernike optimization by iteratively imposing different Zernike modes (OSA/ANSI indices 3 through 14) on the DM and adopting the amplitudes that maximize coupling into the SMF.

We conduct a throughput experiment to measure the spatial sensitivity of the DAFN system to off-axis planet light. The procedure we follow is similar to the experiment outlined in Ref. 8. The nulling SMF is translated to measure coupling efficiency as a function of angular separation. When the fiber is on-axis with the optical

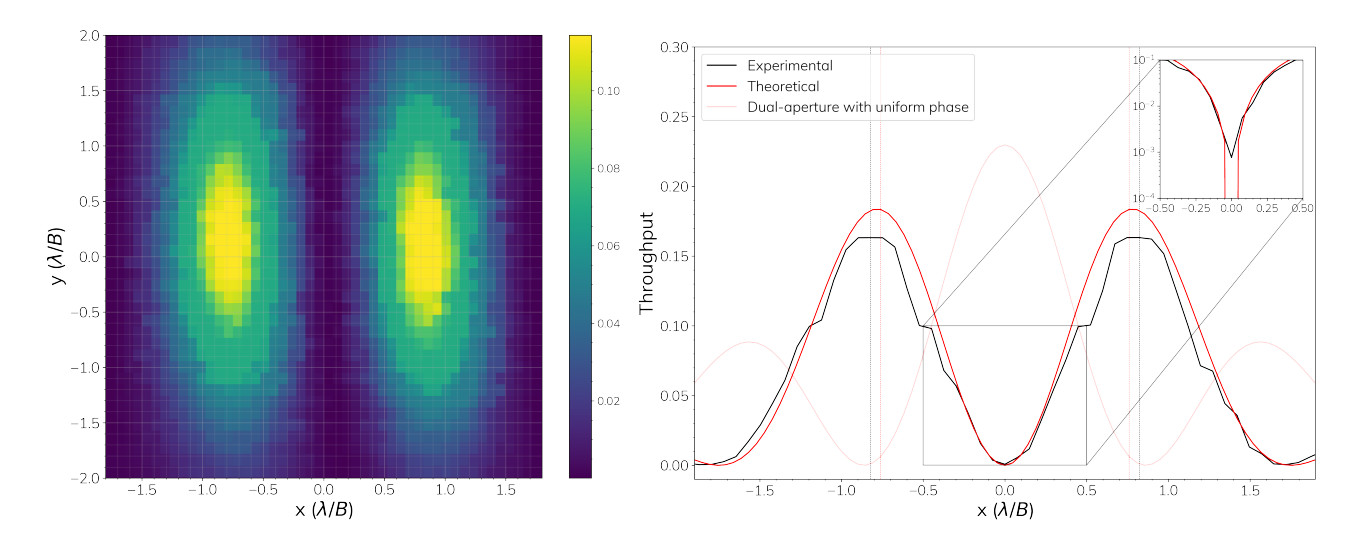


Figure 3. (Left) 2D DAFN coupling map. (Right) 1D throughput scan through DAFN null in black, with theoretical limits for reference in red.

path, this configuration measures the degree of starlight suppression or null depth. Since the PSF of the system does not change morphology with a shift of the source, translating the nulling fiber is equivalent to translating source fiber off-axis to simulate planet light. To maintain alignment of upstream optics, we choose to translate the nulling fiber to simulate off-axis coupling from a companion planet. A peak in the coupling efficiency map corresponds to the separation at which off-axis planet light throughput is maximized. This experiment allows us to constrain both the angular separation at which an off-axis companion source can be detected as well as the null depth and correspondingly a laboratory estimate of contrast sensitivity.

#### 3. RESULTS

Figure 3 shows the preliminary results of the DAFN throughput experiment from our testbed. The 2D coupling map on the left matches the anticipated morphology with two bright fringes at separations less than  $1\lambda/B$ .

The right figure shows a 1D scan through the null. We achieve 16.3% peak throughput (see the black curve) of off-axis planet light, less than 2% off from the theoretical maximum shown by the red curve. Planet light coupling peaks near  $\sim 0.75 \lambda/D$ , very close to expectations from theoretical simulations as indicated by the proximity between the black (experiment) and red (theory) dashed vertical lines. Such small IWAs can enable direct detection of planets with the contrasts and separations of hot Jupiters (P < 10 days, a  $\sim 0.05$  AU).

We measure null depth as the brightness ratio between the on-axis dark fringe (see the minimum of the black curve in the inset) and off-axis bright fringes (peaks of the black curve). Our best measured null depth is  $4.67 \times 10^{-3}$ . The measured null depth is consistent with the 0.1- $0.125 \lambda$  wavefront error estimated from the difference between the measured ( $\sim 64\%$ ) and theoretical (80.6%) peak coupling efficiency of the unmasked beam into the SMF, as well as the wavefront error measured from the OAPs. This suggests that there are wavefront aberrations in the system that require correction for improved starlight suppression. This will likely require fine-tuning the optical alignment since we have maximized utility of the DM with our Zernike optimization procedure. We are working towards null depths of  $\sim 10^{-5}$  as attained in complementary laboratory fiber nuller demonstrations in monochromatic light<sup>8-10</sup> to enable detection of giant planets in reflected light.

#### 4. ONGOING WORK

To push for deeper nulls, we will work on refining the optical alignment of our testbed and scanning the DM through a range of offsets near the nominal value for a  $\pi$  phase shift between the two apertures.

To test DAFN sensitivity to low-order perturbations, we will use the DM to inject different Zernike mode wavefronts simulating stellar light leakage and measure null depth as a function of Zernike mode amplitude.

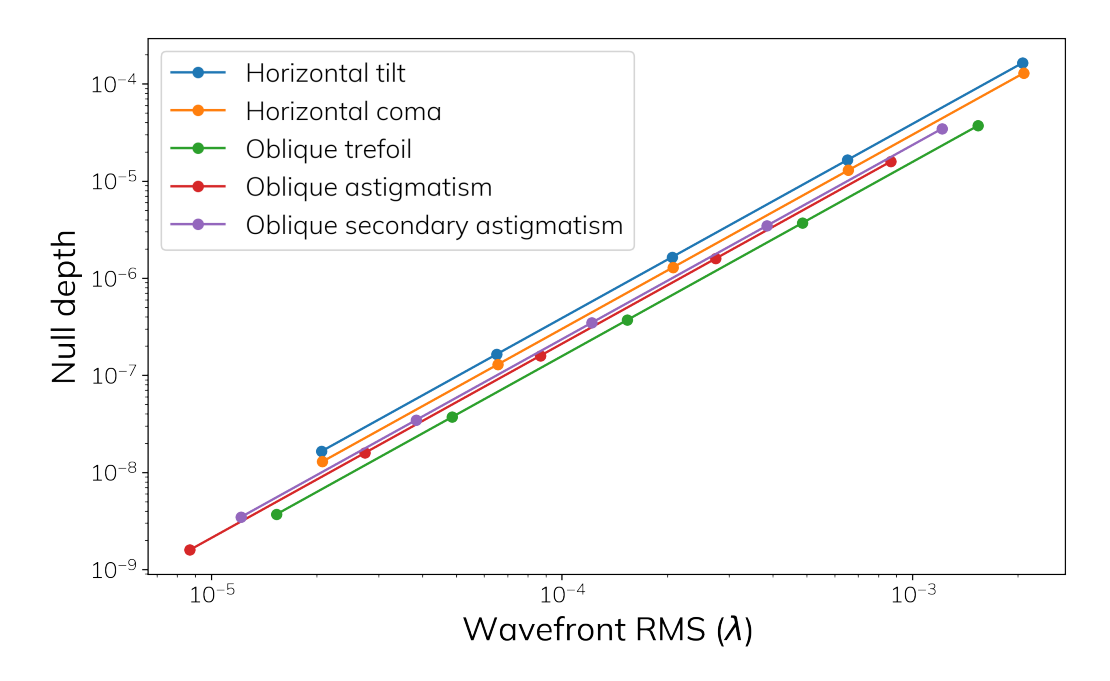


Figure 4. Null depth sensitivity to different Zernike modes that most strongly deteriorate DAFN performance.

Figure 4 shows how (simulated) null depth degrades with different Zernike modes to which the DAFN is most sensitive. DAFN performance is strongly responsive to Zernike aberrations that break lateral symmetry across the two apertures, i.e. horizontal and oblique modes rather than vertical modes.

## 5. CONCLUSION

We present preliminary results from a monochromatic DAFN testbed in optical light. We achieve sub- $\lambda/D$  sensitivity to off-axis light with  $\sim 5 \times 10^{-3}$  null depths. From estimates of wavefront error in the system, we expect improvements in optical alignment will help deepen the null. Once we optimize null depth and off-axis throughput, we will test DAFN sensitivity to Zernike mode aberrations. In the future, we plan to upgrade the testbed to broadband optical light, then a near-infrared source and a spectrometer on the backend for applications in observing chemical tracers of planet formation (carbon/oxygen/nitrogen/sulfur-bearing molecules) and potential biosignatures. Exciting potential avenues for this testbed include concept demonstrations of the next generation of multi-aperture nulling interferometry instruments for the LBT, VLT, and upcoming missions like LIFE.

## ACKNOWLEDGMENTS

A.P.A would like to thank the NASA Space Technology Graduate Research Opportunity for aiding and funding the work presented, as well as the AstroTech program for supporting her initial efforts in instrumentation. The authors extend gratitude to Dr. Daniel Echeverri, Yinzi Xin, Dr. Nemanja Jovanovic, Prof. Dimitri Mawet, and Dr. Eugene Serabyn for their insightful consultation, especially to members of Prof. Mawet's lab group who assisted with a preliminary demonstration of this experiment on the PoRT testbed at Caltech. Finally, the authors thank Jon Shover, Jerry Mason, Mike Engelman, and Prof. Rick Pogge at The Ohio State University's Imaging Sciences Lab for assisting with logistical matters and manufacturing custom parts for the testbed.

# REFERENCES

[1] Bracewell, R. N., "Detecting nonsolar planets by spinning infrared interferometer," **274**, 780–781 (Aug. 1978).

- [2] Kaltenegger, L. and Fridlund, M., "The darwin mission: Search for extra-solar planets," *Advances in Space Research* **36**, 1114–1122 (01 2004).
- [3] Lawson, P., Lay, O., Martin, S., Beichman, C., Johnston, K., Danchi, W., Gappinger, R., Hunyadi, S., Ksendzov, A., Mennesson, B., Peters, R., Scharf, D., Serabyn, E., and Unwin, S., "Terrestrial planet finder interferometer: 2006-2007 progress and plans," 8 (09 2007).
- [4] Hanot, C., Mennesson, B., Martin, S., Liewer, K., Loya, F., Mawet, D., Riaud, P., Absil, O., and Serabyn, E., "Improving Interferometric Null Depth Measurements using Statistical Distributions: Theory and First Results with the Palomar Fiber Nuller," 729, 110 (Mar. 2011).
- [5] Serabyn, E., Mennesson, B., Martin, S., Liewer, K., and Kühn, J., "Nulling at short wavelengths: theoretical performance constraints and a demonstration of faint companion detection inside the diffraction limit with a rotating-baseline interferometer," 489, 1291–1303 (Oct. 2019).
- [6] Echeverri, D., Xuan, J., Jovanovic, N., Delorme, J.-R., Ruane, G., Hillman, S., Mawet, D., Wallace, J. K., Mennesson, B., and Millar-Blanchaer, M., "First light of the vortex fiber nulling mode on the Keck planet imager and characterizer," in [Techniques and Instrumentation for Detection of Exoplanets XI], Ruane, G. J., ed., 12680, 126800M, International Society for Optics and Photonics, SPIE (2023).
- [7] Wang, J. and Jurgenson, C., "Exoplanet Sciences with Nulling Interferometers and a Single-mode Fiber-fed Spectrograph," 160, 210 (Nov. 2020).
- [8] Echeverri, D., Ruane, G., Jovanovic, N., Mawet, D., and Levraud, N., "Vortex fiber nulling for exoplanet observations I Experimental demonstration in monochromatic light," *Optics Letters* 44, 2204 (May 2019).
- [9] Haguenauer, P. and Serabyn, E., "Deep nulling of laser light with a single-mode-fiber beam combiner," 45, 2749–2754 (Apr. 2006).
- [10] Serabyn, E., Liewer, K., and Ruane, G., "Geometric-phase-based phase-knife mask for stellar nulling and coronagraphy," *Optics Express* **32**, 19924 (May 2024).